AIAA JOURNAL
Vol. 33, No. 9, September 1995

Simulation of Overexpanded Low-Density Nozzle Plume Flow

Chan-Hong Chung*
NASA Lewis Research Center, Cleveland, Ohio 44135
Kenneth J. De Witt†
University of Toledo, Toledo, Ohio 43606
and
Robert M. Stubbs‡ and Paul F. Penko§
NASA Lewis Research Center, Cleveland, Ohio 44135

The direct simulation Monte Carlo method was applied to the analysis of low-density nitrogen plumes exhausting from a small converging–diverging nozzle into finite ambient pressures. Two cases were considered that simulated actual test conditions in a vacuum facility. The numerical simulations readily captured the complicated flow structure of the overexpanded plumes adjusting to the finite ambient pressures, including Mach disks and barrel-shaped shocks. The numerical simulations compared well to experimental data of Rothe.

Introduction

IN contrast to the behavior of low-density plumes expanding into a vacuum, the flow expanding into a region of finite pressure is often overexpanded with a more complicated flow pattern involving Mach disks and shock waves. Under these conditions, the supersonic flow can be confined to a narrow core, depending on the applied background pressure, and the sonic line may not intersect with the nozzle lip as it does with a vacuum ambient, in which case the external conditions can influence the internal flow through the thick subsonic region near the nozzle wall.

Low-density flow through small nozzles expanding to vacuum has been examined previously in both experimental and numerical investigations, although, little experimental data are available and most data are for gross characteristics of nozzle performance such as thrust and discharge coefficients. Data that provide detailed information on internal flow structure were published by Rothe,[1,2] in which density and rotational temperature distributions were measured inside a small nozzle and in the nozzle plume using the electron-beam fluorescence technique. Rothe's experiment was numerically simulated by Chung et al.[3] using a continuum code based on the Navier–Stokes equations and the direct simulation Monte Carlo (DSMC) method of Bird.[4] The simulation results were compared with Rothe's density and rotational temperature data at various locations inside the nozzle and at the nozzle exit plane. In this study, no consideration was given to simulation of the finite test-facility pressure. In somewhat related work, pitot pressure measurements and numerical simulations were made for a low-density nozzle and plume flow by Penko et al.[5] and Boyd et al.[6] Comparisons were made between continuum and DSMC results and pitot pressure measurements at the nozzle exit plane and various locations in the plume. Comparisons of continuum and DSMC results were also made for the flow inside the nozzle. In these works, test-facility pressures were quite low and, therefore, consideration was not given to numerical simulation of the actual ambient pressure. In other work, Campbell et al.,[7] Nelson and Doo,[8] and Zelesnik et al.[9] also analyzed expanding low-density nozzle flows using the DSMC method and compared their results with experimental data.

Presented as Paper 94-0357 at the AIAA 32nd Aerospace Sciences Meeting, Reno, NV, Jan. 10–13, 1994; received March 14, 1994; revision received Feb. 6, 1995; accepted for publication Feb. 15, 1995.

*Resident Research Associate; currently at Department of Chemical Engineering, Taegu University, Kyungbuk, Kyungsan-Gun, 713-714, Republic of Korea. Member AIAA.

†Professor, Department of Chemical Engineering. Member AIAA.

‡Chief, Computational Methods for Space Branch. Member AIAA.

§Aerospace Engineer. Member AIAA.

The rocket engines under consideration typically have thrust levels under 100 mN, are physically small in size, and have relatively low operating pressures and mass flow. Reynolds numbers are low, on the order 10^3, and rarefaction effects are significant. Under these conditions, the flow contains strong nonequilibrium effects, such as slip at a wall, from rapid expansion to near vacuum conditions. The flow transitions from continuum to free-molecular regimes. Conventional continuum gas dynamics may not be adequate to accurately analyze the flow, and an approach based on kinetic theory may be required.

Of the various methods available for analysis of low-density gas flows, the DSMC method is most widely used and readily applicable. The DSMC method is a numerical simulation technique for solving the Boltzmann equation by modeling a real gas flow using a representative set of molecules. Theoretically, the DSMC method can be applied to any flow for which the Boltzmann equation is valid, but intensive computational requirements generally restrict the use to near continuum and rarefied flows. Continuum methods are usually much more efficient than the DSMC method for higher density flows. Thus, in the analysis of flows which involve both continuum and rarefied regimes, it is reasonable to apply both methods. The simplest utilization of both methods is to solve the rarefied flow regime with the DSMC method using boundary conditions for the inflow surface obtained from the continuum method used to solve the continuum and near-continuum regime.

In this paper, the DSMC method is employed for the analysis of low-density nitrogen flows expanding through a small converging–diverging nozzle and into finite back pressures that simulate Rothe's experimental conditions. Special attention is given to the effect of the nonzero ambient pressure on the flow structure, both in the nozzle and, especially, in the plume, to simulate conditions often encountered in ground-based test facilities used to test small thrusters. These conditions are illustrated in the results from the numerical simulation and in comparison with Rothe's experimental data.

Problem Statement

Rothe's experiment[2] was chosen as a reference problem because of the availability of detailed measurements. Figure 1 illustrates the geometry of the nozzle used in Rothe's experiment and in the numerical simulation. The actual nozzle was made of graphite to reduce optical reflections and to minimize backscattering and secondary emission of electrons. The subsonic and supersonic portions of the nozzle are cones having half-angles of 30 and 20 deg, respectively, with longitudinal radii of curvature at the throat equal to one-half of the throat radius. The area ratio at the exit based on the throat area is 66. The shaded region in Fig. 1 indicates the domain of the DSMC simulation. The length of the curved contour downstream of the throat (IH) is about 0.5 mm. The simulation domain extends

Table 1 Flow conditions

	Case I	Case II
Test gas	N_2	N_2
Stagnation temperature T_0, K	300	300
Stagnation pressure P_0, Pa	474	1245
Ambient pressure P_b, μHg	11	28.5
Wall temperature T_w, K	300	300
Reynolds number Re_t	270	709
Knudsen number Kn	2.3×10^{-3}	8.8×10^{-4}

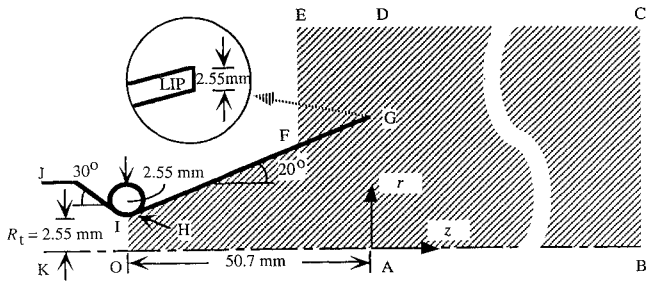

Fig. 1 Geometry of low-thrust nozzle.

from the throat to an axial distance 260 mm from the nozzle exit plane (AB), a radial distance 50 mm from the nozzle lip (GD), and an axial distance 20 mm from the nozzle exit plane into the backflow region (DE). The inflow boundary is located at the nozzle throat (OI). The boundary condition at the inflow boundary is obtained from a solution of the Navier–Stokes equations.[3] The radial boundary CE is located far enough from the axis so that extending it farther radially does not result in any significant changes in the macroscopic flow variables in the plume. Along the boundaries CE and EF, an equilibrium condition corresponding to the ambient gas is used as the boundary condition. Likewise, the downstream boundary BC is located far enough from the nozzle exit so that extending it farther downstream does not result in any significant changes in the macroscopic flow variables in the near plume. Along the boundary BC, several boundary conditions are tested including an equilibrium condition corresponding to the ambient condition, a vacuum boundary condition, and an equilibrium condition corresponding to a profile extrapolated from the inside of the plume. The test gas is nitrogen with a stagnation temperature of $T_0 = 300$ K. The flow conditions are listed in Table 1. In the table, the throat Reynolds number, $Re_t = 2\dot{m}/\pi\mu_0 R_t$, is based on the viscosity at the stagnation chamber condition μ_0. Here the quantity $\dot{m}$ is the mass flow rate and R_t is the throat radius. The Knudsen number Kn is based on the throat diameter and the stagnation chamber condition.

DSMC Method

The DSMC code used in this study is based on the principles described by Bird,[4] together with the variable hard sphere (VHS) model[10] as a molecular model and the no time counter (NTC) method[11] as a collision sampling technique. The code was developed to investigate various low-density flows of gas mixtures in arbitrarily shaped flow domains.[3,12,13] Details of the code may be found in Ref. 3. The execution speed of the code for the flow considered in this study, measured by CPU time/particle/times step, is about 1.3 μs on a Cray Y-MP. The flow domain consists of about 20,000 cells in 41 subregions. At the steady phase of the simulation, the total number of simulated molecules in the flow domain is about 2×10^6. The flowfield is sampled every 5 time steps during 20,000 time steps after reaching the steady phase. The total CPU time required for the computation is about 19 h on the Cray Y-MP.

The VHS exponent ω of nitrogen is chosen to be 0.24 with the reference molecular diameter of 4.07×10^{-10} m at the reference temperature 273 K (Ref. 10). Chemical reactions and the vibrational mode are assumed to be frozen. For the calculation of the rotational energy exchange between the colliding molecules, the Borgnakke–Larsen[14] phenomenological model is employed together with the temperature-dependent energy exchange probability of Boyd[15] modified by Chung et al.[3] to be consistent with the experimental data for the rotational relaxation of nitrogen obtained by various methods and compatible with the VHS model. A diffusely adiabatic wall with 10% thermal accommodation is assumed for the interaction between the gas molecules and the wall, which shows the best agreement with the measured rotational temperature.[3] Although not shown, gas/surface interaction models have a negligible effect on the flow property near the axis of the nozzle except for the specular reflection that results in a faster expantion of the flow. A detailed description of the effect of gas/surface interaction models can be found in Ref. 3.

To assess the effect of backscattering of downstream molecules and reduce the number of simulated molecules, the gas is treated as a mixture consisting of two different nitrogen sources whose origins are the upstream reservoir and the downstream, respectively. A ratio of the actual to the simulated molecules for the nitrogen whose origin is the downstream is chosen to be four times larger than that for the nitrogen coming from the upstream reservoir.

Results and Discussion

To present the general idea of the overexpanded plumes the pressure distribution will be considered first. The pressure distribution along the axis of the nozzle is depicted in Fig. 2, which shows the extent of overexpansion in the plume. It can be seen in the figure that even in case I the flow is slightly overexpanded just outside the nozzle exit, where the minimum pressure is about 73% of the ambient pressure. However, the overexpansion is not strong enough to cause any significant disturbances in the flow. In case II, the centerline pressure at the exit is already 60% of the ambient pressure and drops to 33% of the ambient pressure at 25 mm downstream from the exit. Hence, back-pressure effects cause the flow to turn into the axis and produce the characteristic barrel-shock configuration. Beyond the shock, the flow continues to expand. In this case, however, the expansion is not sufficiently strong to sustain the repetitive pattern of compression and expansion. The local Knudsen number distribution along the axis of the nozzle is depicted in Fig. 3, which shows the degree of plume rarefaction. The local Knudsen number is based on the nozzle exit diameter. The local Knudsen numbers in the plume are on the orders of 10^{-1} and 10^{-2} for cases I and II, respectively.

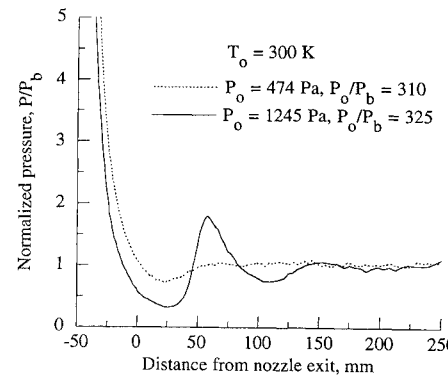

Fig. 2 Pressure distribution along the axis.

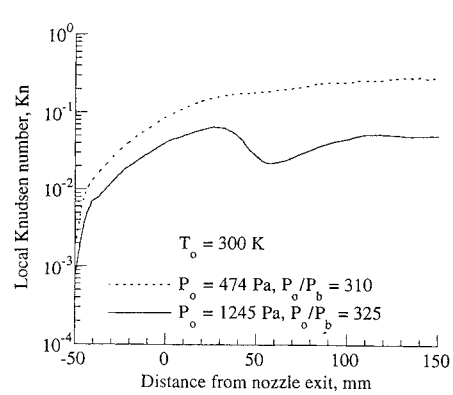

Fig. 3 Local Knudsen number distribution along the axis.

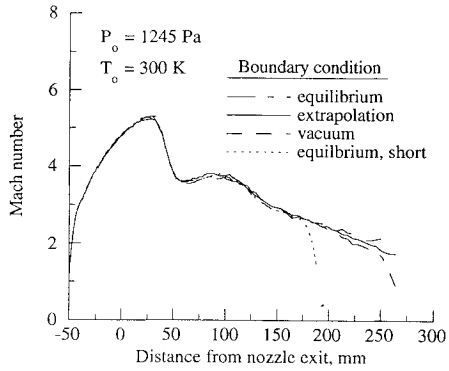

Fig. 4 Mach number distribution along the axis.

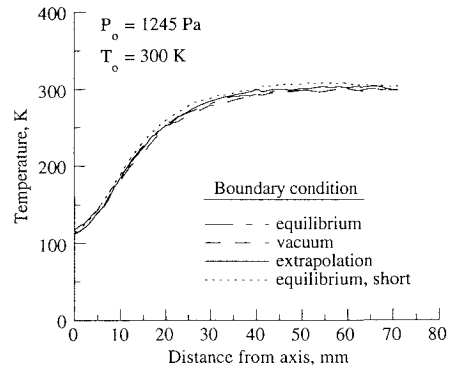

Fig. 5 Translational temperature distribution at z = 150 mm.

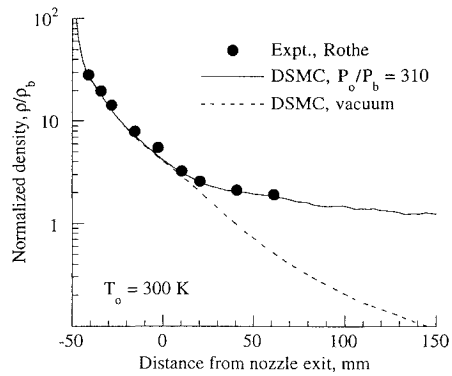

Fig. 6 Density distribution along the axis for P_0 = 474 Pa.

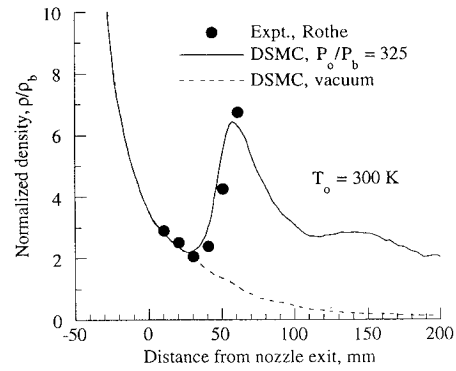

Fig. 7 Density distribution along the axis for P_0 = 1245 Pa.

Consideration is now given to the effect of boundary conditions. For the simulation of nozzle flows with nonzero ambient pressures a supersonic outflow boundary condition, which is usually assumed along boundaries in the simulation of nozzle flows expanding into a vacuum, can not be used since the flow is not supersonic along the boundaries in the plume. The best way would be to extend the simulation domain sufficiently far so that the flow along the boundaries is not disturbed by the expanding plume, and an equilibrium condition corresponding to the ambient gas may be used as the boundary condition, which, unfortunately, is computationally prohibitive. In the present study, the extension of the simulation domain to a radial distance 70 mm from the axis and to an axial distance 20 mm from the nozzle exit plane into the backflow region is found to be sufficient to impose the equilibrium condition corresponding to the far-field ambient condition. It is also found that the extension of the simulation domain to the downstream axial distance 260 mm from the nozzle exit plane is sufficient to resolve important characteristics of the plume.

Figure 4 shows the effect of the boundary condition along the downstream boundary on the centerline Mach number. Two distinctively different boundary conditions are imposed along the downstream boundary at z = 260 mm, including an equilibrium condition corresponding to the ambient condition (dot-dashed line) and a vacuum boundary condition (dashed line). For a third condition, since the radial distribution of flow variables are very similar far downstream, profiles are extrapolated from the inside of the plume, and an equilibrium condition corresponding to the profiles is employed as the boundary condition (solid line). For the sake of comparison, the result obtained by reducing the axial distance from the nozzle exit to the downstream boundary to about 180 mm and imposing an equilibrium condition corresponding to the ambient condition is also shown (dotted line). It can be seen that extremely different boundary conditions have no significant effect on the Mach number distribution in the near plume within 150 mm from the nozzle exit. Figure 5 shows the effect of the boundary condition on the radial translational temperature profile at the axial location z = 150 mm. Again it can be seen that extremely different boundary conditions along the downstream boundary have no significant effect on the radial temperature distribution in the near plume within 150 mm from the nozzle exit, where the most important and distinctive characteristics of the present overexpanded plume occurs. Although not shown, the effect of the boundary conditions on the other flow variables such as density, velocity, and rotational temperature is similar to those observed in Figs. 4 and 5.

The comparison of the simulation results with Rothe's experimental data[2] is made in Fig. 6 in which density profiles along the nozzle axis inside the nozzle and in the plume for case I are shown. The densities are normalized by the ambient density ρ_b. The solid line is from the DSMC simulation with the ambient pressure, and the filled circles represent the experimental data of Rothe. For comparison, a calculation made for the flow expanding into a vacuum is also shown in the figure and is represented by the dotted line. The simulation results indicate that for the two different ambient conditions, the density profiles along the axis show no significant differences inside the nozzle for the case where the stagnation pressure P_0 = 474 Pa. The simulation result with the nonzero ambient pressure shows good agreement with the experimental data both inside the nozzle and in the plume. Figure 7 shows the comparison of the simulation results with experimental data along the nozzle axis for case II where P_0 = 1245 Pa. The density decreases from the throat to the nozzle exit before the shock occurs. The local minimum density is about 2.2 times the ambient density and occurs about 25 mm downstream from the exit. The local maximum density is about 6.4 times the ambient density and occurs about 60 mm downstream from the exit. The density profile along the axis with a nonzero ambient pressure and that for a vacuum ambient show no significant differences before the shock for this case. The simulation result with the nonzero ambient pressure shows good agreement with the experimental data across the shock except for the slight shift in the axial direction.

Comparison of calculated radial density profiles with Rothe's experimental data at various axial locations in the plume for cases I and II are shown in Figs. 8 and 9, respectively. Again, the solid line is the simulation result with nonzero ambient pressure and the filled circles represent the experimental data. The densities are normalized by the ambient density ρ_b. The radial density profiles are arranged in a sequence corresponding to axial positions in the plume. At the lower stagnation pressure of P_0 = 474 Pa, the density profiles have

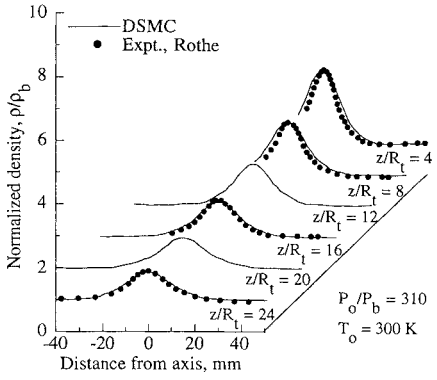

Fig. 8 Comparison of radial density distribution for P_0 = 474 Pa.

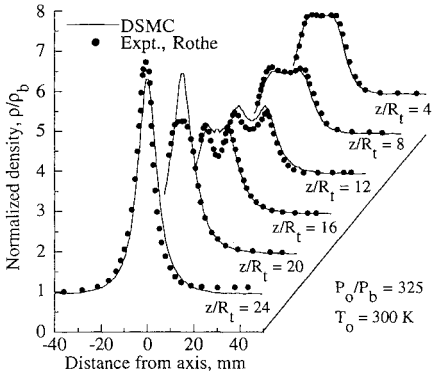

Fig. 9 Comparison of radial density distribution for P_0 = 1245 Pa.

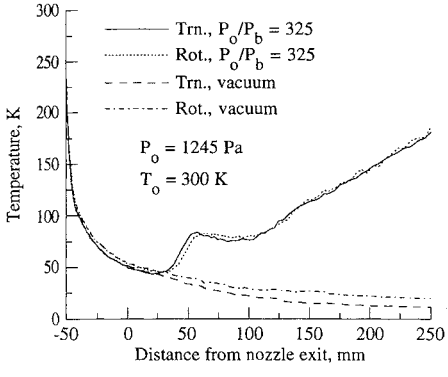

Fig. 10 Temperature distribution along the axis.

a single peak, which decrease both in the radial and axial directions. At the higher stagnation pressure of P_0 = 1245 Pa, the density profiles in the plume are double peaked and indicate the presence of a barrel-shaped shock. The barrel-shaped shock converges to a single density peak farther downstream. In both cases, the jet is confined to a narrow core the diameter of which is about the same as the nozzle exit diameter. The simulation results show good agreement with the experimental data in both cases except for the region around the shock in the higher pressure case where a small difference in the axial location results in a significant difference in the profile as shown in Fig. 7.

The degree of thermal nonequilibrium in the plume is shown in Fig. 10 where both translational and rotational temperature distributions along the axis for case II are plotted. For comparison, temperature distributions for the flow expanding into a vacuum are also shown in the figure. From the rapid expansion, the rotational temperature is higher than the translational temperature along the axis inside the nozzle and in the near plume. In the case of the flow expanding into a vacuum, the two temperatures are frozen far downstream. For the case of the nonzero ambient pressure, however, the translational temperature becomes higher than the rotational temperature across the shock wave from the rapid compression. Beyond the

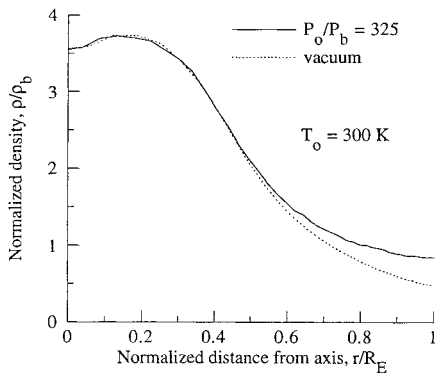

Fig. 11 Density distribution at exit plane for P_0 = 1245 Pa.

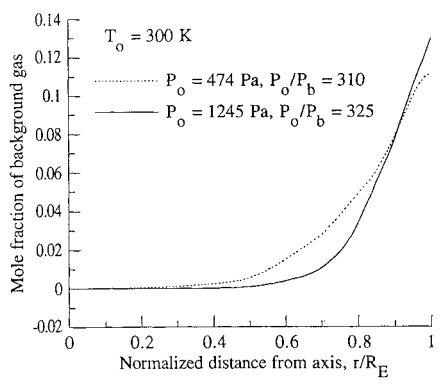

Fig. 12 Mole fraction of ambient gas at exit plane.

shock, the rotational temperature is higher than the translational temperature where the flow once again expands. Far downstream, the two temperatures become the same as the flow approaches equilibrium.

Finally, the effect of the nonzero ambient pressure on the exit plane density is shown in Figs. 11 and 12. In the figures, the quantity R_E is the exit radius of the nozzle. Figure 11 shows the exit plane density profiles for the stagnation pressure P_0 = 1245 Pa. Near the axis, the two densities are nearly the same and are not influenced by the external condition, whereas near the nozzle lip, the effect of the external condition becomes significant. At the nozzle wall, the density of the flow expanding into vacuum is 55% of that with the nonzero ambient pressure. Figure 12 shows the mole fraction of the background gas at the exit plane. It can be seen that near the axis the gas is composed of gas molecules exclusively coming from the upstream stagnation chamber. Near the nozzle lip, a significant number of gas molecules from the ambient have penetrated inside the nozzle. At the lip, the fraction of gas originating from the background gas is about 11 and 13% for cases I and II, respectively.

Conclusions

The flow structure in low-density plumes expanding through a small converging–diverging nozzle into a region of finite pressure is investigated using the DSMC method based on molecular gas dynamics. This kind of flow structure has rarely been studied using the DSMC method. The calculated results show that the plume structure with a nonzero ambient pressure is substantially different from that of the flow expanding into a vacuum. The simulation results show good agreement with Rothe's experimental data measured at various axial and radial locations in the plume. It is shown that the DSMC method can successfully predict the complex flow structures, such as Mach disk and barrel-shaped shock which are representative of overexpanded nozzle plumes.

Acknowledgment

Support for the first author (C. Chung) by the NASA Lewis Research Center, Cleveland, Ohio, under NASA Contract NCC 3-171 is gratefully acknowledged.

References

[1]Rothe, D. E., "Electron Beam Studies of Viscous Flow in Supersonic Nozzles," *AIAA Journal*, Vol. 9, No. 5, 1972, pp. 804–811.

[2]Rothe, D. E., "Experimental Study of Viscous Low-Density Nozzle Flows," Cornell Aeronautical Lab., Inc., AI-2590-A-2, Buffalo, NY, June 1970.

[3]Chung, C. H., Kim, S. C., Stubbs, R. M., and De Witt, K. J., "Low-Density Nozzle Flow by the Direct Simulation Monte Carlo and Continuum Methods," *Journal of Propulsion and Power*, Vol. 11, No. 1, 1995, pp. 64–70.

[4]Bird, G. A., *Molecular Gas Dynamics*, Oxford Univ. Press, London, 1976.

[5]Penko, P. F., Boyd, I. D., Meissner, D. L., and De Witt, K. J., "Pressure Measurements in a Low-Density Nozzle Plume for Code Verification," AIAA Paper 91-2110, June 1991.

[6]Boyd, I. D., Penko, P. F., Meissner, D. L., and De Witt, K. J., "Experimental and Numerical Investigations of Low-Density Nozzle and Plume Flows of Nitrogen," *AIAA Journal*, Vol. 30, No. 10, 1992, pp. 2453–2461.

[7]Campbell, D. H., Wysong, I. J., Weaver, D. P., and Muntz, E. P., "Flowfield Characteristics in Free Jets of Monatomic and Diatomic Gases," *Rarefied Gas Dynamics*, edited by B. D. Shizgal and D. P. Weaver, Vol. 158, Progress in Astronautics and Aeronautics, AIAA, Washington, DC, 1994, pp. 90–97.

[8]Nelson, D. A., and Doo, Y. C., "Simulation of Multicomponent Nozzle Flows into a Vacuum," *Rarefied Gas Dynamics*, edited by E. P. Muntz, D. P. Weaver, and D. H. Campbell, Vol. 116, Progress in Astronautics and Aeronautics, AIAA, Washington, DC, 1989, pp. 340–351.

[9]Zelesnik, D., Dunn, T., Micci, M. M., and Long, L. N., "Numerical and Experimental Investigation of Low Reynolds Number Nozzle Flows," AIAA Paper 91-3558, Sept. 1991.

[10]Bird, G. A., "Monte Carlo Simulation in an Engineering Context," *Rarefied Gas Dynamics*, edited by S. S. Fisher, Vol. 74, Pt. 1, Progress in Astronautics and Aeronautics, AIAA, New York, 1981, pp. 239–255.

[11]Bird, G. A., "The Perception of Numerical Methods in Rarefied Gas Dynamics," *Rarefied Gas Dynamics*, edited by E. P. Muntz, D. P. Weaver, and D. H. Campbell, Vol. 118, Progress in Astronautics and Aeronautics, AIAA, Washington, DC, 1989, pp. 211–226.

[12]Chung, C. H., Kim, S. C., Stubbs, R. M., and De Witt, K. J., "Analysis of Plum Backflow Around a Nozzle Lip in a Nuclear Rocket," AIAA Paper 93-2497, June 1993.

[13]Chung, C. H., Kim, S. C., De Witt, K. J., and Nagamatsu, H. T., "Numerical Analysis of Hypersonic Low-Density Scramjet Inlet Flow," *Journal of Spacecraft and Rockets*, Vol. 32, No. 1, 1995, pp. 60–66.

[14]Borgnakke, C., and Larsen, P. S., "Statistical Collision Models for Monte Carlo Simulation of Polyatomic Gas Mixture," *Journal of Computational Physics*, Vol. 18, No. 4, 1975, pp. 405–420.

[15]Boyd, I. D., "Analysis of Rotational Nonequilibrium in Standing Shock Waves of Nitrogen," *AIAA Journal*, Vol. 28, No. 11, 1990, pp. 1997–1999.